environmental microbiology

Environmental Microbiology (2019) **21**(2), 814–826 doi:10.1111/1462-2920.14515

Chromomycin, an antibiotic produced by *Streptomyces flavisclerotic*us might play a role in the resistance to oxidative stress and is essential for viability in stationary phase

Divya Prajapati,[1] **Namita Kumari**,[2†] **Keyur Dave**,[3†] **Vaidehi Chatupale**[1] **and Jayashree Pohnerkar**[1*]

[1]*Department of Bio-Chemistry, The Maharaja Sayajirao University of Baroda, Baroda, 390003, Gujarat, India.*

[2]*Center for Sickle Cell Disease, Howard University, Washington, DC, 20059.*

[3]*Cellcys Labs Pvt. Ltd., Mumbai, 400104, India.*

Summary

The well-known role of antibiotics in killing sensitive organisms has been challenged by the effects they exert at subinhibitory concentrations. Unfortunately, there are very few published reports on the advantages these molecules may confer to their producers. This study describes the construction of a genetically verified deletion mutant of *Streptomyces flavisclerotic*us unable to synthesize chromomycin. This mutant was characterized by a rapid loss of viability in stationary phase that was correlated with high oxidative stress and altered antioxidant defences. Altered levels of key metabolites in the mutant signalled a redistribution of the glycolytic flux toward the PPP to generate NADPH to fight oxidative stress as well as reduction of ATP-phosphofructokinase and Krebs cycle enzymes activities. These changes were correlated with a shift in the preference for carbon utilization from glucose to amino acids. Remarkably, chromomycin at subinhibitory concentration increased longevity of the non-producer and restored most of the phenotypic features' characteristic of the wild type strain. Altogether these observations suggest that chromomycin may have antioxidant properties that would explain, at least in part, some of the phenotypes of the mutant. Our observations warrant reconsideration of the secondary metabolite definition and raise the possibility of crucial roles for their producers.

Received 12 October, 2017; revised 13 December, 2018; accepted 20 December, 2018. *For correspondence. E-mail jayashreepohnerkar@hotmail.com; Tel. +91-9426760232; Fax +91-0265-2792277. †N.K. and K.D. have contributed equally to this work.

Introduction

*Streptomyces flavisclerotic*us is a member of the genus *Streptomyces* that are ubiquitous, filamentous gram positive soil bacteria which are obligatory aerobes. *Streptomycetes* are well-known for their ability to produce a wide range of bioactive compounds including antibiotics. However, the function of these so called secondary or specialized metabolites in the physiology of the producing bacteria remains enigmatic. The concept of antibiotics as toxic molecules secreted by an organism for a competitive advantage has prevailed for a long time, and therefore, other potential roles have remained unexplored (Vining, 1990). However, since the 1990s, additional biological effects of antibiotics beyond biological warfare have been discovered (Davies, 1990; Demain and Fang, 2000). In their natural habitat, most of antibiotics are produced at subinhibitory concentrations and it is now recognized that antibiotics trigger concentration-dependent phenotypic responses, e.g., a hormetic effect (Davies *et al*., 2006; Yim *et al*., 2006). Only very few studies report the direct function of antibiotics for the producing organism. Phenazines synthesized by *Pseudomonas aeruginosa*, have important role in the physiology of the producer including impacts on central carbon metabolism (Price-Whelan *et al*., 2007), iron acquisition, maintenance of the intracellular redox homeostasis and intercellular signalling (Price-Whelan *et al*., 2006). Myxovirescin, an antibiotic produced by *Myxococcus xanthus* was shown to play a role in the virulence of this bacteria (Xiao *et al*., 2011). Furthermore, recent studies demonstrate concentration-dependent pro- and antioxidant effects of some antibiotics (Lertvorachon *et al*., 2005; Leirós *et al*., 2013), this effect being potentially pertinent to human health applications. Indeed, several important functions of secondary metabolites have been discovered in studies designed to screen for metabolites possessing human medicinal value besides their antibiotic

function. For instance, the aromatic polyketide chromomycin and minocycline were shown to possess neuroprotective properties (Kraus *et al*., 2005; Jain, 2011) but chromomycin was also reported to interact strongly with DNA and inhibits transcription and replication (Menendez *et al*., 2004). Other functions of molecules belonging to the aureolic class of compounds that includes chromomycin, are reviewed (Lombo *et al*., 2006; Jain, 2011).

In this article, we describe the beneficial effects that sublethal concentrations of chromomycin (Fig. 1A) have

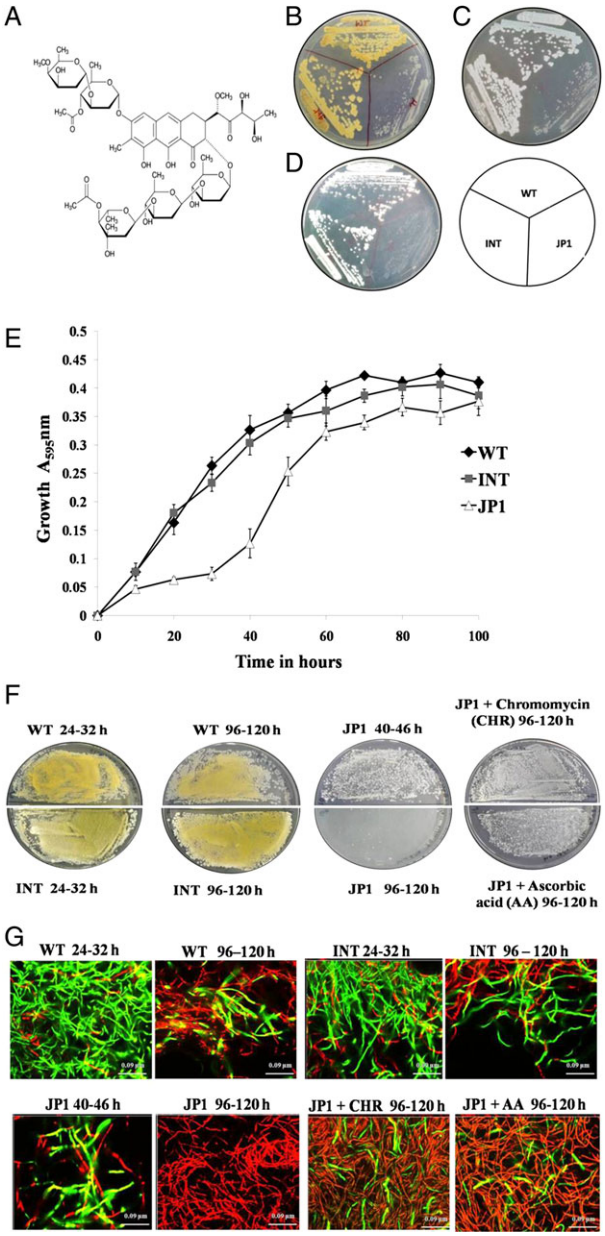

Fig. 1. Growth characteristics and viability of chromomycin non-producer JP1 mutant, and restoration of its viability by *ex vivo* supplementation of chromomycin and ascorbic acid.

A. Structure of chromomycin A3 (Figure source: Sigma); (B) Deletion mutant (JP1) does not produce yellow fluorescent antibiotic chromomycin on R2YE and grows slowly; (C) exhibits complete absence of sporulation on R2YE; (D) does not grow on minimal media (R4) containing glucose as sole carbon source; in contrast INT (integrant) and wild type (WT) are indistinguishable with respect to all the phenotypes; (E) Growth curve of wild type, JP1 and INT cells grown in TSB was measured by DNA (A_{595} nm) estimation. The results are representative of three independent experiments and the error bars represent mean ± SD; (F) Growth phase dependent viability of cells of WT, INT and JP1 and restoration of viability of JP1 mutant in stationary phase by subinhibitory concentration of chromomycin and ascorbic acid as measured by plating on R2YE (undiluted). The plate pictures are representative of several plating experiments; (G) representative view of staining of WT, INT, JP1 and JP1 cells treated with chromomycin and ascorbic acid by Live/Dead Baclight Kit; and visualization under LSM – 710 confocal microscope. Hours of growth are as indicated. The experiments were repeated more than three times.

on the life span of its producer, *S. flaviscleroticus.* We also revealed that the antibiotic has important impacts on the physiology and the metabolism of its producer. The various phenotypes of the non-producing mutant include (i) growth retardation, (ii) precocious drop of the viability of cells in early stationary phase, (iii) increase of internal oxidative stress, (iv) metabolic readjustments such as the reorientation of the glycolytic flux toward PPP and reduced ATP-phosphofructokinase and Krebs cycle enzymes activities and (v) a shift in the preference for the utilization of carbon source from glucose to amino acids. Altogether these data suggest that chromomycin possesses antioxidant properties. Indeed, providing subinhibitory concentrations of chromomycin to the mutant led to an increase in the life span of the mutant and restoration of most of the metabolic features of the wild type strain. This study unambiguously demonstrated the importance of chromomycin in the antioxidant defence arsenal of its producer and thus in the survival of the latter. Our results also confirmed the intimate link existing between oxidative stress and the life span of a prokaryote.

Results and discussion

Deletion mutant lacking chromomycin genes exhibits pleiotropic phenotypes

The details of the construction of the genomic library of *S. flaviscleroticus* and its genomic mutant, JP1, are provided in Supporting Information Text S1 in the Supporting Information Figs. S1–S3. The 12 kb DNA fragment (Gene Bank Accession No. KC249518.1) deleted from the mutant strain (JP1) carries genes for minimal PKS and modifying enzymes (Supporting Information Fig. S1 and Table S1).

The deletion of this fragment abolishes the strain's ability to produce chromomycin and was associated with unexpected phenotypes. These phenotypes include (i) twofold reduction in the growth rate of the mutant (Fig. 1B and E); (ii) early loss of viability (Fig. 1F and G); (iii) complete absence of sporulation (Fig. 1C) and (iv) absence of growth on minimal medium with glucose as sole carbon source (Fig. 1D).

These phenotypes could not be inferred from the genetic information residing in the deleted 12 kb DNA fragment. Indeed, bioinformatics analysis of the genes carried by the 12 kb DNA fragment deleted in the mutant revealed a close match of these genes with those of the chromomycin biosynthetic gene cluster of *S. griseus* subsp. *griseus* (Menendez *et al*., 2004) known to be involved in antibiotic biosynthesis.

The complementation of the JP1 mutant by introduction of the PKS genes carried by the #2.19 cosmid integrated into the chromosome of the latter (integrant-INT) restored wild type features ruling out the possible occurrence of secondary mutations responsible for the phenotypes of the JP1 mutant.

Growth of the chromomycin non-producer JP1 mutant is slower than that of wild type and it loses viability early in stationary phase

Growth of the JP1 mutant was markedly slower than that of the wild type strain on rich R2YE agar medium (Fig. 1B) as well as in liquid trypton soya broth (TSB) (Fig. 1E). In TSB the JP1 mutant shows a longer lag and grows twofold slower than the wild type strain. On the basis of its DNA content analysis, it is delayed approximately 8–10 h in comparison with the WT and INT strains (Fig. 1E).

Since in the model organisms *E. coli* and *S. cerevisiae*, a decrease in the plating efficiency of stationary phase cells is thought to be due to damage to the macromolecular machinery linked to increased oxidative stress leading to reduced life span (Nystrom, 1999; Fredriksson and Nystrom, 2006), we monitored the viability of stationary phase cells of the JP1 mutant strain compared with the WT and INT strains. Two methods were used to do so: (i) plating on R2YE agar and counting the colonies present in 0.1 ml of culture harvested at different times (ii) staining the live/dead cells using the fluorescent nucleic acid dyes, Syto9 and propidium iodide, that stain in green or red the live and dead cells respectively (BacLight kit, Invitrogen). We are aware that, considering the mycelial growth of *Streptomyces*, assessing the viability of a *Streptomyces* culture by the plating method is only an approximation of the number of viable cells. However, this method is useful for a continuous assessment of colony forming ability of the culture over several days of incubation (Fig. 1F). Live/dead staining of cells shown in Fig. 1G indicated that WT, INT (24–32 h) and JP1 (40–46 h) strains contain approximately 80%–90% viable cells. Plating 0.1 ml culture of each strain produced a confluent lawn that was considered to be 100% viable. The viability of the JP1 begins to diminish after 72 h of growth. After 96–120 h of growth, the WT and INT contain approximately 50% of the red (dead) and green (live) stained cells in striking contrast with JP1 whose most cells were stained red, indicating dead cells (Fig. 1G). The same pattern was reflected in the plating experiment. The loss of viability of the WT and INT was 10-fold lower than the radical loss of viability of the JP1 culture after 96 h of cultivation (<0.01% living cells, Fig. 1F). The *in vivo* impact of chromomycin was tested by its ability to reverse/correct the phenotypes of the JP1 mutant strain. We incorporated in the growth medium chromomycin or the antioxidant ascorbic acid at subinhibitory concentrations (Supporting Information Text S1) and monitored viability. The characteristic rapid

and early loss of viability of the mutant was reversed to a significant extent by the addition of chromomycin at subinhibitory concentrations (Fig. 1F and G). This was evidenced by a > 50-fold greater number of colonies in the culture treated with chromomycin (Fig. 1F) and the significant increase in the number of stained green living cells (Fig. 1G). A comparable reversal in the loss of viability of the mutant at stationary phase was also observed with ascorbic acid, a proven antioxidant of nonbacterial origin (Fig. 1F and G).

Deletion of chromomycin biosynthesis genes is associated with high oxidative stress in the JP1 mutant

Oxidative stress constitutes the 'Achilles heel' that determines the viability and life span of any organism utilizing O_2 as a terminal electron acceptor. Reactive Oxygen Species (ROS) such as superoxide anion radical (O_2^-), hydrogen peroxide (H_2O_2) and the highly reactive hydroxyl radicals ($^{\cdot}OH$) generate oxidative stress. To combat this stress, the cell induces several antioxidant enzymes such as catalase, hydroperoxidase or superoxide dismutase. However, if the generation of oxidants exceeds the antioxidant defences of the cells, accelerated aging, decreased viability and deleterious effects on life span are observed (Nyström, 2004). In order to determine whether the early loss of viability of the JP1 mutant was linked to oxidative stress, we quantified and compared the activity of various antioxidant enzymes (catalase, hydroperoxidase and superoxide dismutase) in the WT, INT and JP1 mutant strains every 24 h after inoculation (Figs 1F and G and 2A). The catalase activity slowly increased in the WT (and INT) from ~30 h onward, peaked at 72–80 h, and then gradually decreased over the next 48 h (120 h) (Fig. 2A). The pattern of catalase activity was correlated with viability as measured by plating (Fig. 1F). In contrast, the catalase activity in JP1 peaked at 40–46 h, then decreased continuously over the next 60–80 h. Interestingly, the catalase activity pattern was also correlated with the viability of the JP1 strain; the number of viable cells reaching its maximum after 40 to 72 h of growth and was then drastically reduced after 96 h of cultivation (Figs 1F and 2A). The decrease in the total catalase activity of JP1 at stationary phase is also reflected in a higher concentration of extracellular H_2O_2 production as measured by an amplex red horseradish peroxidase assay (Fig. 2B).

Subsequently, considering that 24–32 h and 50–60 h represented mid-log and stationary phases of growth for WT and INT, respectively, whereas 40–46 h 70–80 h represented mid-log and stationary phases for the JP1 mutant strains (Fig. 1E), we measured the expression levels of four different catalase encoding genes identified in the genome of *S. flavisclerotic*us (Supporting Information Text S1) using semi quantitative RT-PCR. We showed that the transcripts of the H_2O_2-inducible catalases (Fig. 2C), *cat1* and *cat2*, were more abundant in mid-log phase than in stationary phase cells of the JP1 mutant (Fig. 2D) whereas *cat3* expression was undetectable in JP1 in both growth phases (Fig. 2D). In contrast, the expression of the three catalases was higher in stationary phase than in the mid-log phase, in the WT and INT strains. At last, the expression of the putative manganese-dependent catalase, *cat4*, was not detectable during any phase of growth in any of the three strains (data not shown). The transcriptional pattern of expression of different catalase genes is thus consistent with the characteristic pattern of the total enzymatic activity of the WT, INT and JP1 strains.

Interestingly, the supplementation of subinhibitory concentrations of chromomycin during growth enhanced the activity and expression of different catalase genes at stationary phase in the JP1 mutant strain (Fig. 2E). This was correlated with the restoration of the expression of *cat1* and *cat2* in stationary phase (Fig. 2F).

Similarly, the activity of the alkyl hydroperoxidase was twofold higher in the JP1 mutant than in the WT and INT strains in the mid-log phase and decreased in stationary phase (Fig. 2G). Consistently, the decrease in the catalase/hydroperoxidase activity of stationary phase cells of the JP1 mutant was correlated with a higher sensitivity to 100 mM H_2O_2 than mid-log phase cells of this strain (Fig. 2H). In contrast, the total SOD activity was found to be similar in the three strains in both mid-log and the stationary phases (Fig. 2I), suggesting that the oxidative stress in JP1 may not involve superoxide radicals.

Interestingly, fluorescence of the DCFDA dye, sensitive to oxidation by ROS, was almost twofold higher in the JP1 mutant strain than in the WT and INT strains suggesting that the JP1 mutant was probably under constitutive oxidative stress (Fig. 2J). Consistently, the *in vitro* fluorescence of DCFDA in cell-free extracts of the JP1 mutant strain was also higher than that of the WT strain extracts (data not shown). Since it was reported that DCFDA fluorescence could be used as a reporter of the redox reactions linked to intracellular iron (Kalyanaraman *et al*., 2012), we cannot exclude that chromomycin plays a role in iron homeostasis, since it is known to bind iron and other divalent metals (Kamiyama, 1968).

External supplementation of chromomycin at subinhibitory concentration in the course of the growth of the JP1 mutant was correlated with a reduction of DCFDA fluorescence (Fig. 2K), of extracellular production of H_2O_2 (Fig. 2L).

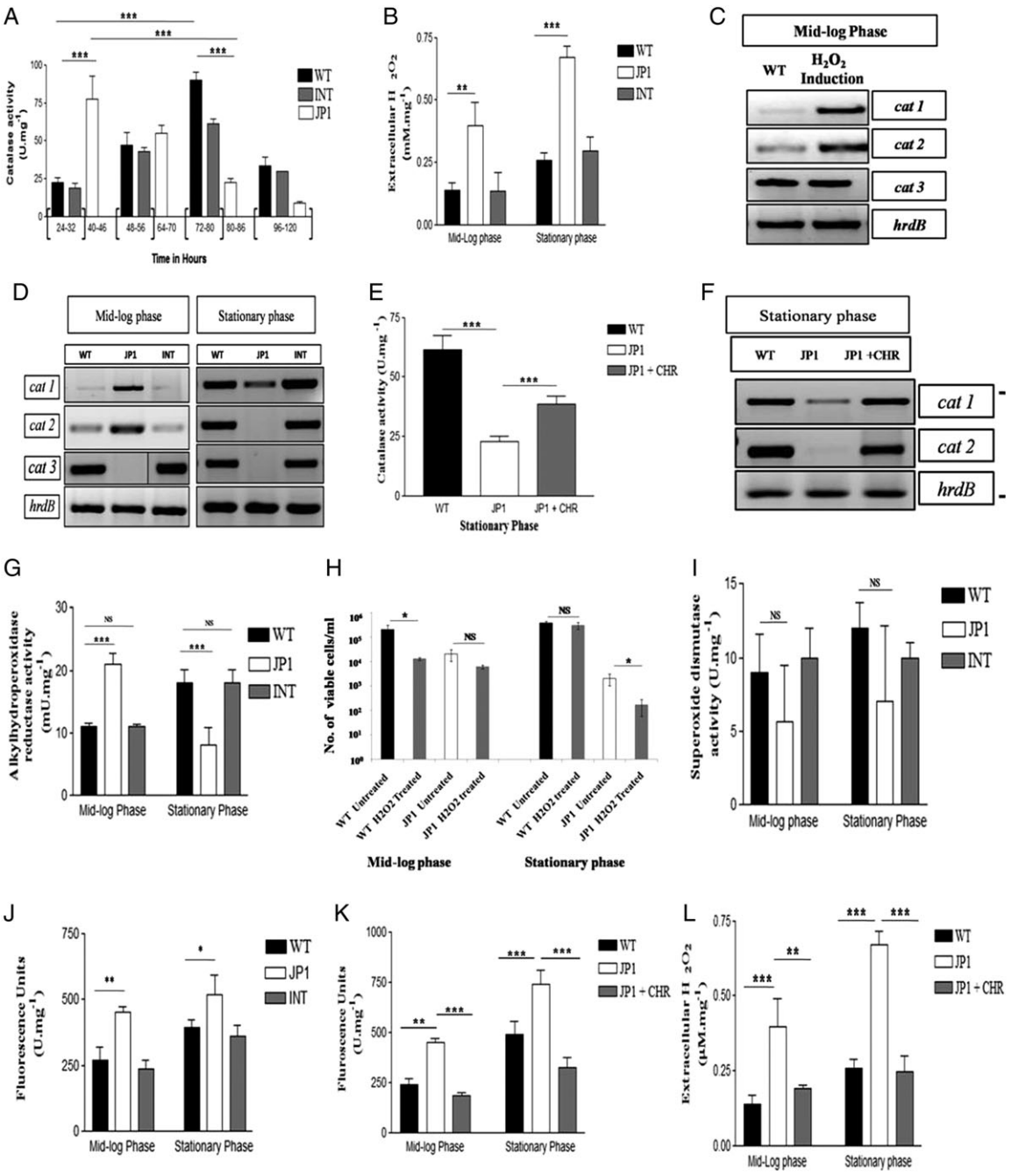

Fig. 2. The JP1 mutant exhibits enhanced oxidative stress corrected by *ex vivo* supplementation of chromomycin at subinhibitory concentration. A. status of the antioxidant enzyme catalase in the JP1 mutant; (B) extracellular production of H_2O_2, estimated by Amplex Red-HRP in cells of WT, INT and JP1 in mid-log and in stationary phase of growth; (C) transcription analysis of catalase genes, *cat1* through *cat3* by semi quantitative RT-PCR of RNA extracted from cells of WT, INT and JP1 mutant in mid-log and stationary phase of growth; (D) transcription analysis of induction of *cat1* and *cat2* in mid-log phase culture of WT treated with 100 mM H_2O_2 for 2 h. The transcription profiles are representative of three independent experiments**.** Agarose gel electrophoresis image processed by ImageJ software; (E) increase in the total catalase activity in the stationary phase of the JP1 mutant treated with chromomycin; (F) *cat* transcript levels are more pronounced in the cells treated with chromomycin in stationary phase; (G) alkyl hyroperoxidase enzyme activity monitored at different phases of growth in WT, INT and JP1; (H) Sensitivity of JP1 mutant to killing by H_2O_2 in mid-log and in stationary phase; (I) total SOD levels monitored at different phases of growth in WT, INT and JP1 (specific enzyme activity expressed as units mg^{-1} protein); (J) Total ROS measured by DCFDA fluorescent probe; (K) decrease in intracellular ROS levels in JP1 mutant treated with chromomycin; (L) reduction in extracellular production of H_2O_2 (as measured in B) in chromomycin treated culture of JP1. Results are representative of three independent experiments and error bars represent mean ± SD. Statistically significant differences between strains at each time point were assessed by one-way ANOVA followed by post hoc test (Tukey test; GraphPad Prism) $^*p < 0.05$, $^{**}p < 0.01$, $^{***}p < 0.001$.

Table 1. Assessing *in vitro* antioxidant and iron–reducing property of chromomycin.

	Ascorbic acid	Chromomycin	Tetracyclin
DPPH assay IC50 (50% Scavenging activity) in μg	7.7	28	141
FRAP assay FRAP Value in μM	2	0.7166 7 ± 0.05	0.0766 ± 0.02
Ferric Ferrozine Assay Total antioxidant capacities (TAC) mM trolox-equivalent	1.1×10^{-2}	2.8×10^{-3}	4.1×10^{-4}

It is well-known that oxidative stress triggers the induction of specific enzymes involved in the resistance to oxidative stress in various microorganisms (Imlay, 2008, 2013). Consequently, the early expression of these enzymes in the JP1 mutant indicates that it suffers from early oxidative stress. We propose that the absence of chromomycin is responsible for this early oxidative stress in the JP1 mutant suggesting that chromomycin fulfils an anti-oxidant function. The extracellular supplementation of chromomycin can largely reverse the obvious effects of oxidative stress (Fig. 2E, F, K and L).

Chromomycin acts as an antioxidant in vitro

In order to assess the antioxidant properties of chromomycin and determine whether its absence could lead to the high oxidative stress of the chromomycin non-producer mutant JP1, we assessed its antioxidant potential with three different methods: (i) the 1,1-diphenyl-2-picrylhydrazyl (DPPH) assay. It measures the hydrogen donating ability of the antioxidant to the stable DPPH radical, (ii) the FRAP assay in which the reducing power of the electron-donating antioxidant leads to a change in the colour of ferric-tripyridyl triazine (FeIII TPTZ, straw colour) complexed to its ferrous form (blue colour) that is monitored at 593 nm, (iii) the ferric ferrozine assay is performed at a physiological pH (Berker *et al*., 2010) and thus more relevant for measuring the antioxidant property of a compound, unlike the FRAP method in which highly unrealistic pH (pH 3.6) may suppress the reducing capacity of antioxidant compounds due to their protonation. The outcome of these assays was compared with that of standard molecules, ascorbic acid and tetracycline. Chromomycin scored as a better antioxidant than tetracycline with all three assays (Table 1). The results of these assays indicate that chromomycin has *in vitro* antioxidant and iron binding/reducing activity that could have important *in vivo* implications.

Chromomycin non-producer mutant of S. flaviscleroticus *is characterized by upregulation of PPP enzymes and downregulation of glycolytic and Krebs cycle enzymes*

A reorientation of the glycolytic flux toward PPP is known to be necessary to generate NADPH to combat oxidative stress in *Pseudomonas fluorescens* (Mailloux *et al*., 2011). Indeed, the conversion of fructose-6-phosphate to 6-phosphogluconate catalysed by G6PDH (*zwf*) and the conversion of the latter into ribulose-5-phosphate catalysed by the 6-phosphogluconate dehydrogenase (6-PGDH) generates NADPH (Berg *et al*., 2002).

In order to determine whether the high oxidative stress of the JP1 mutant (Fig. 2) was correlated with a similar rewiring of its metabolism, we determined the activity of the G6PDH and the 6-PGDH. These activities were ~ twofold higher (Fig. 3A and B) and the NADPH levels were also ~2.5-fold higher (Fig. 3C and D; Supporting Information Fig. S4) in the JP1 mutant strain than in the WT and INT strains. A higher transcriptional activity of both *zwf1* and – *2* genes in JP1 mutant strain than in the WT strain is consistent with the higher activity of these enzymes (Fig. 3E).

To demonstrate that the enhancement in the carbon flow into the PPP pathway was achieved at the expense of glycolysis, we assayed the activity of the 6-phosphofructokinase (PFK), the first committed enzyme of glycolysis that catalyses a rate limiting step and has an important regulatory role (Berg *et al*., 2002). The PFK encoding genes of *S. flavisclerotic*us were found by comparing its genome sequence with that of other *Streptomyces* species (see Supporting Information Text S1). We assayed individually the activity of the ATP-PFK and PPi-PFK enzymes from cell-free extracts of the WT, INT and JP1 mutant strains (Borodina *et al*., 2008). The PPi-dependent activity of PFK (PFK2) was undetectable (data not shown) whereas the levels of the ATP-dependent enzyme (PFK3) were reduced by more than twofold in JP1 compared with the WT and INT strains (Fig. 3F). This reduced activity coincided with the reduced transcript levels of the *pfk3* gene (Fig. 3G) whereas the transcript of the second putative ATP-dependent *pfk1* was undetectable in both the WT, INT and JP1 mutant strains (data not shown). The decrease in the total PFK activity in the JP1 mutant is thus likely to be primarily due to the reduced transcription of *pfk3.* The reduction in the channelling of glucose through glycolysis may have affected the levels of the end-product acetyl-CoA accordingly, the amounts of this metabolite in JP1 were reduced twofold relative to the WT, as measured by HPLC (Fig. 3H and Supporting Information Fig. S5).

Furthermore, since TCA cycle generates reduced co-factor that donate electrons to the respiratory chain, it is also potentially involved in ROS generation. Consequently,

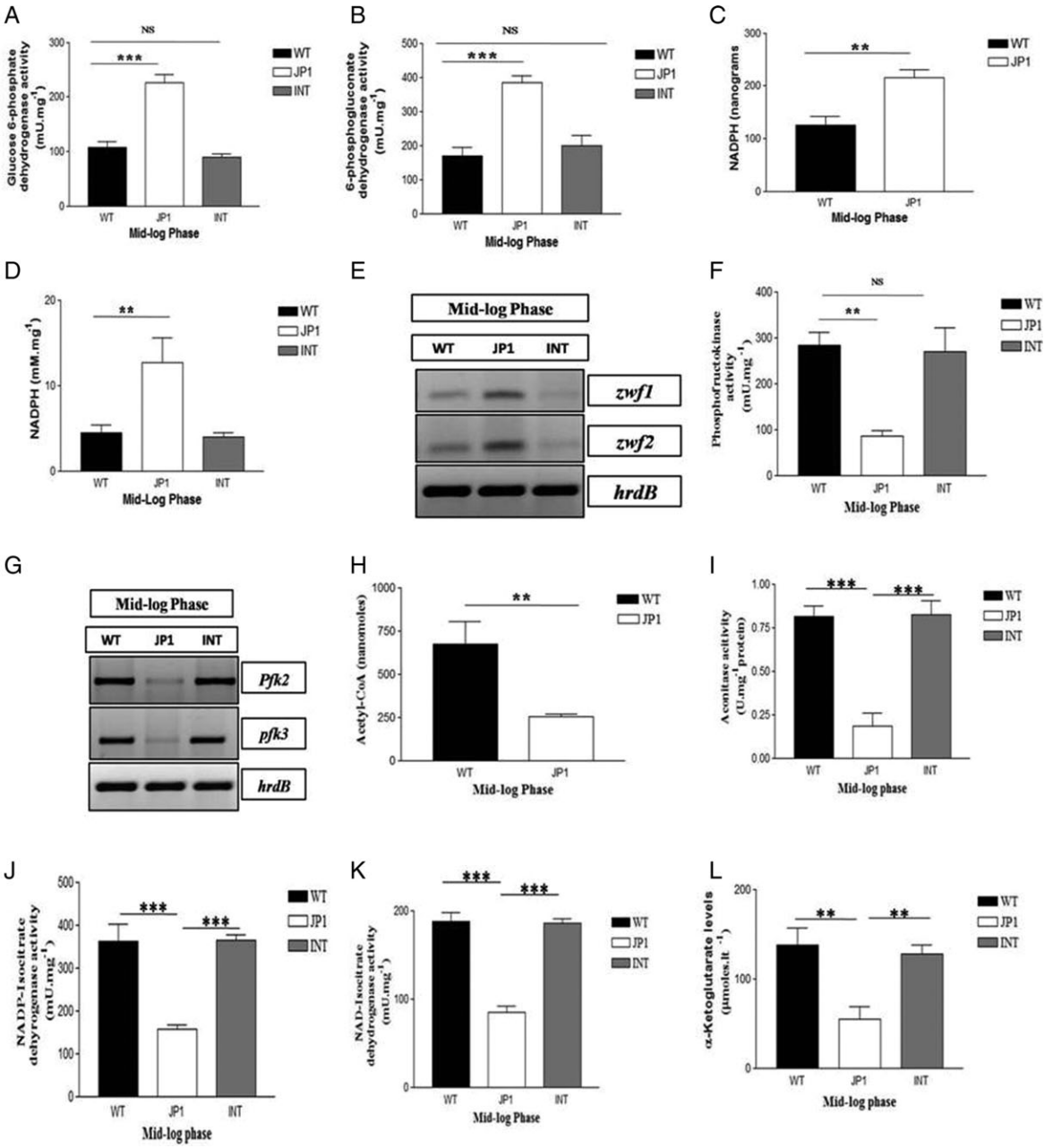

Fig. 3. The alterations in central carbon metabolism in JP1 mutant.
The measurement of enzyme activities (specific activity -units mg^{-1} protein), metabolite analyses and expression analyses were performed with cultures of WT, INT and JP1 grown to mid-log phase. Results are representative of three independent experiments (A) G6PDH- and (B) 6-PGDH enzyme activities; Intracellular levels of NADPH compared by (C) HPLC and (D) enzymatic cycling method; (E) semi quantitative RT-PCR analysis of *zwf1* and – *2***.** Agarose gel electrophoresis image processed by ImageJ software; (F) ATP-PFK activity; (G) semi quantitative RT-PCR analysis of ATP-*pfk* (*pfk3*) and PPi-*pfk* (*pfk2*). Agarose gel electrophoresis image processed by ImageJ software; (H) measurement of intracellular levels of acetyl Co-A in cells of WT and JP1 by HPLC. The TCA cycle enzyme activities were assayed for (I) Aconitase; (J) NADP – Isocitrate dehydrogenase (ICDH); (K) NAD – Isocitrate dehydrogenase (ICDH); (L) α-ketoglutatrate levels; error bars represent mean ± SD. Statistically significant differences between strains at each time point were assessed by one-way ANOVA followed by post hoc test (Tukey test; GraphPad Prism3) for multiple comparisons and unpaired *t*-test *$p < 0.05$, ** $p < 0.01$.

the downregulation of enzymes of the Krebs cycle generating NADH is consistent with the adjustments required to limit ROS generation and thus oxidative stress (Nyström, 2004; Imlay, 2008). We thus assayed the enzymatic activities of aconitase (Acn) and isocitrate dehydrogenase (ICDH) in the three strains. These activities were twofold to fourfold lower in the JP1 mutant strain than in the WT and INT strains (Fig. 3I–K). The levels of

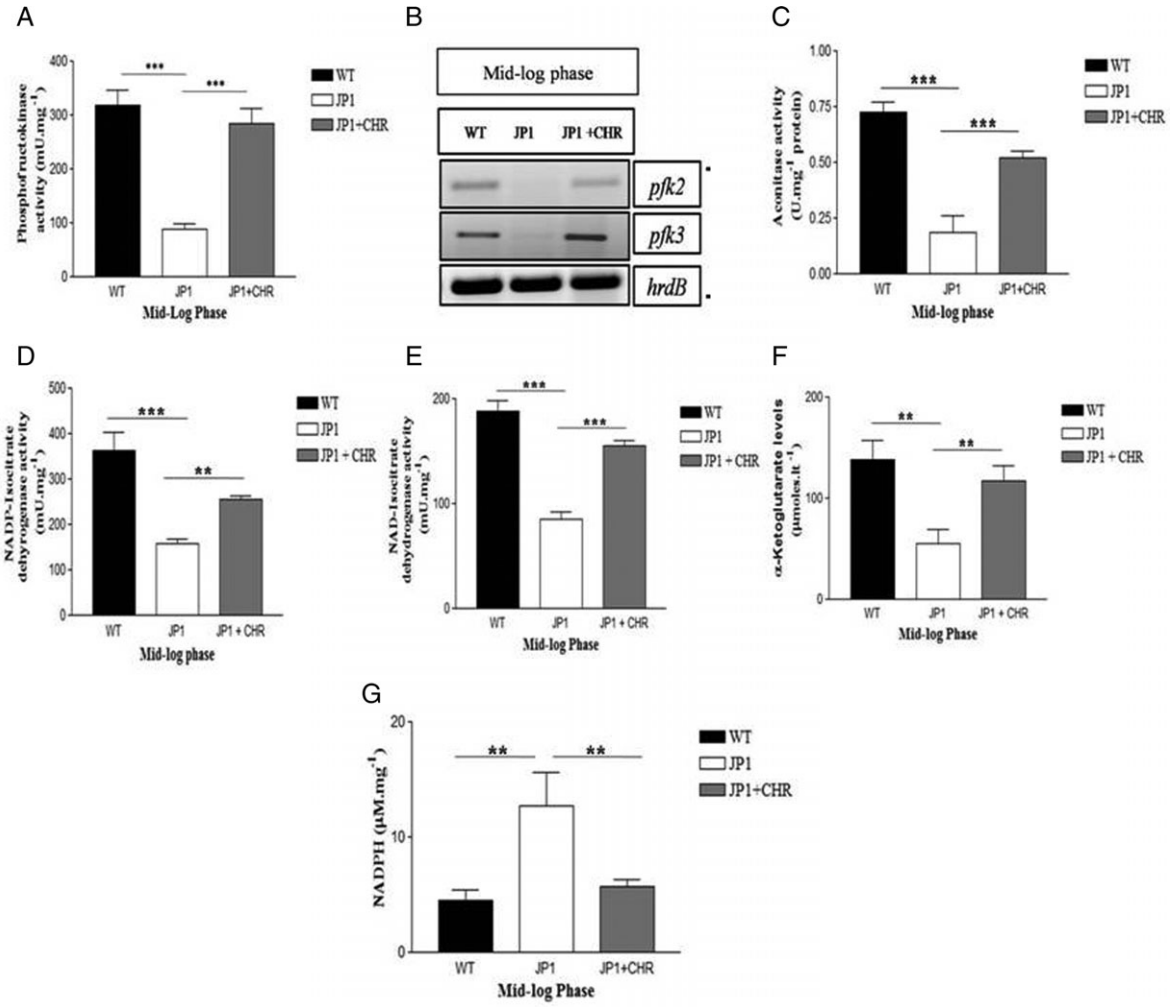

Fig. 4. The restorative effects of sublethal concentration chromomycin on central carbon metabolism in JP1.
Restoration of (A) ATP-PFK activity; (B) *pfk* transcript levels; Kreb cycle enzyme activities for (C) aconitase; (D) NADP-IDH; (E) NAD-IDH and metabolites, (F) α-ketoglutarate levels; (G) intracellular levels of NADPH as measured by enzymatic cycling method in JP1. The results are representative of three independent experiments; error bars indicate mean ± SD. Statistically significant differences between strains at each time point were assessed by one-way ANOVA followed by post hoc test (Tukey test; GraphPad Prism3) for multiple comparisons and Student's *t*-test ***$p < 0.001$, **$p < 0.01$.

α-KG, the entry point of nitrogen in the metabolism and a proposed antioxidant (Lemire *et al*., 2010), were similarly twofold lower in JP1 than in the WT and INT strains (Fig. 3L). These features might contribute to the slow growth of the mutant.

Interestingly, the supplementation of subinhibitory concentrations of chromomycin during growth enhanced ATP-PFK activity (Fig. 4A) twofold to threefold in comparison with the JP1 culture grown in its absence. Semi quantitative RT-PCR analysis of the *pfk* genes expression indicated that the expression of *pfk3* encoding ATP-PFK, was significantly enhanced in the cells of JP1 treated chromomycin while the *pfk2* transcript was only marginally affected (Fig. 4B). The activities of TCA cycle enzymes (aconitase, NAD- and NADP-IDH) and the levels of the metabolite α-ketoglutarate were augmented in the cells of JP1 grown in the presence of sublethal concentration of chromomycin (Fig. 4C–F). Consistent with the reduction in measures of oxidative stress (Fig. 2E, F, K and L), the levels of NADPH in JP1 mutant treated with sublethal levels of chromomycin were reduced in relation to wild type (Fig. 4G).These effects could well be the indirect consequences of the correction of oxidative stress parameters.

S. flavisclerotic*us preferentially utilizes amino acids as a carbon source over glucose*

*S. flavisclerotic*us exhibits an inherent preference for amino acids as a carbon source over glucose (Fig. 5A). Indeed,

the biomass yield in minimal glucose media is half of that in minimal media containing casamino acids (CAA) as carbon source (Fig. 5A). *Streptomyces fradiae* (Romano and Nickerson, 1958) and *Streptomyces coelicolor* (Millan-Oropeza *et al*., 2017) also preferentially uses amino acids rather than glucose as carbon source but the molecular basis of these metabolic features are not known.

Interestingly, the chromomycin non-producer mutant JP1 did not grow at all on mineral minimal medium containing glucose as the sole carbon source (Figs 1D and 5B) despite the fact that glucose uptake was similarly complete in the WT and JP1 mutant strain at the end of growth (data not shown). The JP1 mutant grew equally well on minimal medium supplemented with 0.5% casaminoacids (CAA) or with a mixture of 20 amino acids at 0.5% with or without added glucose (Fig. 5B). Growth of the JP1 mutant was specifically rescued by the gluconeogenic amino acids that generate α-KG, including glutamate, glutamine, histidine, proline and arginine at concentrations that meet the carbon requirement of JP1 (Fig. 5B). The combination of these five amino acids was better at promoting growth than any individual amino acid. For reasons not yet understood, arginine supplementation is compulsory in combination with the other two or three amino acids whereas none of the remaining 15 amino acids were able to support the growth of the JP1 mutant strain on mineral media (Fig. 5B). We therefore postulate that growth of JP1 could be limited by α-KG availability.

Furthermore, interestingly, the NADPH levels were found to be 40% higher in cells grown in CAA than in those grown in glucose (Table 2) and consistently the glucose-grown cultures of the WT strain were more vulnerable to inhibition by H_2O_2 and diamide (Table 2) than the cells grown in media containing CAA. These high NADPH levels might contribute to the reduction of oxidative stress in the WT strain grown on CAA.

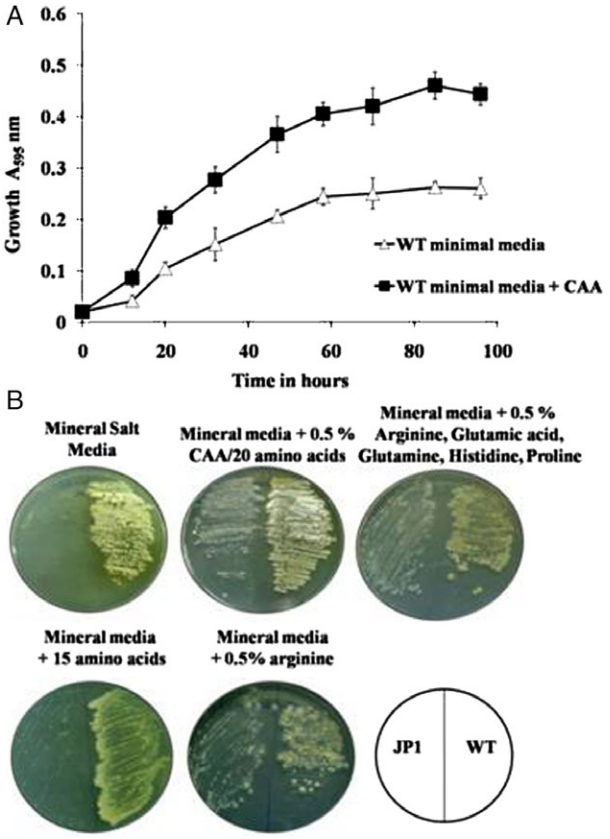

Fig. 5. Inherent preference of WT for amino acids over glucose as a sole carbon source aggravate the growth defect of JP1 mutant on minimal glucose media.
A. Growth curve of WT/INT as measured by DNA estimation (A_{595} nm) in minimal medium with glucose as sole carbon source and in minimal glucose medium with 0.5% CAA as carbon source; (B) Growth of WT and JP1 was compared on mineral salt media/R4 media with supplementations as indicated (C source is glucose and proline, N source is proline and P source is potassium phosphate, C/N ratio of the components of the growth media are provided in the Supporting Information Text S1).

Chromomycin biosynthetic genes are expressed early in exponential phase of growth and induced by H_2O_2 stress

The synthesis of most secondary metabolites usually takes place in stationary phase and to determine whether it was also the case for chromomycin, we assessed the expression of a few representative genes of chromomycin biosynthetic pathway, (i) *sflD*, encoding a NDP- glucose synthase, is the first gene of a four genes operon whereas *sflP* encoding the acetate condensing aglycone synthesis function constitutes the third gene of this operon (ii) *sflMIII* encoding a O-methyl transferase catalyses the late step of chromomycin biosynthesis, (iii) *sflRI*, encodes a putative transcriptional activator and (iv) *sflRII*, encodes a putative repressor that regulates chromomycin biosynthesis (Supporting Information Fig. S1 and Table S1). We observed that the expression of *sflRI*, *sflD* and *sflMIII* was detectable within 12 h after spores inoculation and significantly increased in mid-log phase (27 h) remaining high in stationary phase (60 h/end of the experiment) (Fig. 6A). In contrast, the expression of *sflRII* was detectable at all time points at constant levels (Fig. 6A). Even if the transcriptional profile of all the genes of the cluster was not determined, we believe that these results are significant and reflect the chromomycin biosynthesis potential of the organism in early growth phase as also testified by the yellow colour of the 24 h lawns of. *S. flaviscleroticus* (Fig. 1F). So in contrast to most other secondary metabolites, chromomycin is likely to be produced during the log growth phase of the wild type strain. At early time points (12 h, 17 h, 21 h), chromomycin may be synthesized at sub-MIC (minimum

Table 2. The effect of carbon content of the growth medium on tolerance to oxidative stress.

Growth medium	Diamide		H_2O_2		NADPH levels (mM mg^{-1})
	Diameter (mm)	Surface area (mm^2)	Diameter (mm)	Surface area (mm^2)	
Minimal glucose	20.166 ± 0.28	319.255	20.26 ± 0.46	322.4	1.7 ± 0.15
Minimal glucose + Casamino acids	14.66 ± 0.57	168.86	10.33 ± 0.57	83.82	2.7 ± 0.17

The zone of inhibition of growth and area correspond to that formed by 0.5 M diamide and 0.9 M H_2O_2.
The SD is determined from three independent experiments.

inhibitory concentration) that might affect the physiology of the strain but are presumably insufficient to bind DNA and thus inhibit replication/transcription and finally growth. Treatment of wild type cells grown in TSB broth (~ 28–32 h), at mid-log growth phase, with 50 mM H_2O_2 for 1 h, induced the expression of the putative pathway specific activator *sflRI*, as well as *sflD*, suggesting that the expression of these genes is induced by oxidative stress (Fig. 6B). This suggests that the synthesis of chromomycin constitutes an adaptative response to oxidative stress.

Conclusion

The data presented in this study strongly suggest that chromomycin acts as an antioxidant *in vitro* as *in vivo.* This property explains the pleiotropic phenotypes of the chromomycin non-producer mutant that are mostly reversed by external supplementation of chromomycin with one exception. Indeed, external supplementation of chromomycin did not reverse the growth defect of the JP1 mutant on mineral media with glucose as sole carbon source. This may be due to (i) an inherent preference of *S. flavisclerotic*us for amino acids rather than glucose as carbon source, (ii) reconfiguration/rewiring of carbon metabolism due to constitutive oxidative stress in the JP1 mutant and (iii) the inability of exogenous chromomycin provided during growth to mimic its intracellular regulated production. It should also be mentioned that the chromomycin non- producing mutant of *Streptomyces griseus* sub spp. *griseus* (Menendez *et al*., 2004) does not exhibit the same phenotype as the JP1 mutant of *S. flavisclerotic*us. The reason for this discrepancy is not yet clear. Although there is a remarkable conservation of both the sequence and organization of the genes of the chromomycin biosynthesis gene cluster (Supporting Information Table S1), it is pertinent to note that the ribotyping of the 16S rDNA sequence indicate that the two strains are unrelated (data not shown). Additionally, it is not uncommon that mutations have strain-specific effects in *Streptomyces.* For example, mutations in *pfk2*, *zwf* and *relA* exhibit strain specific effects on antibiotic production (Chakraburtty and Bibb, 1997; Butler *et al*., 2002; Ryu *et al*., 2006; Borodina *et al*., 2008; Gomez-Escribano *et al*., 2008).

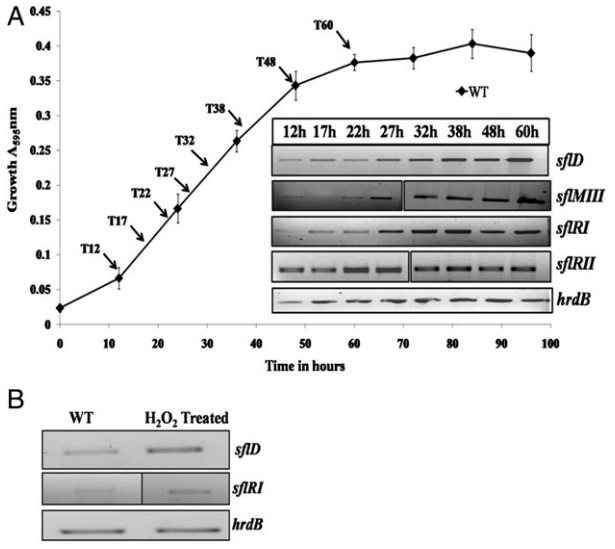

Fig. 6. Early growth phase expression of chromomycin biosynthesis genes in the wild type and their induction by extracellular H_2O_2.
A. Growth by DNA estimation (A_{595} nm) of WT in liquid R2YE medium and expression analysis of representative chromomycin biosynthesis genes. The cells were harvested for the isolation of total RNA at the time points indicated. Stages of growth were defined by changes in DNA content of the cells; (B) Induction by H_2O_2 (50 mM) of early chromomycin biosynthesis gene, *sflD,* representing the transcript of *sflP* (encoding the chromomycin aglycone synthesizing function) and putative activator, *sflRI.* The expression analysis results are representative of three independent experiments.

It is evident from recent bacterial genome sequencing projects that the *Streptomyces* genus harbours a large repertoire of silent/cryptic genes (Rutledge and Challis, 2015; Ochi, 2017) for secondary metabolites, including antibiotics, in addition to the genes expressed under laboratory conditions. Thus, in the natural soil environment, there is a strong possibility that a function of an antibiotic unrelated to its growth inhibitory effect is important for the producer bacterium.

Experimental procedures

Bacterial strains and plasmids used in this study are listed in Supporting Information Table S2. *S. flavisclerotic*us and its derivatives were routinely grown on R2YE and TSB medium (Hi Media). Antibiotics apramycin and thiostreptone were used at 50 μgm ml^{-1} final concentration.

Buffered R4 medium containing either glucose (1%) or casaminoacids (0.5%) was used as minimal medium (Kieser, 2000).

Quantitation of growth by DNA estimation (diphenylamine method), protocols of different enzyme assays, protein estimation, quantitation of intracellular reactive oxygen species, NADPH estimation by enzymatic cycling method and details of RT-PCR are described in Supporting Information Text S1. A list of oligos used in this study is included in Supporting Information Table S3. Normalization of the cultures used for all enzyme assays was carried out considering viability and protein estimation. Enzyme activities are expressed as units/mg protein. Wild-type (and INT) (post 24–32 h) and JP1 (post 40–46 h) cells representing mid-log phase of growth of each, were harvested for the measurement of enzyme activities of antioxidant enzymes (catalase, alkylhydroperoxidase and SOD), glycolytic and TCA enzymes (PFK, aconitase, G6PDH, 6-PGDH and ICDH) and quantitation of metabolites (Acetyl-CoA, α-KG and NADPH). For estimation of antioxidant enzyme activities (catalase, SOD and AHP) in stationary phase cultures, WT and INT each were grown for 50–60 h and JP1 mutant was grown for 70–80 h. The viability of JP1 mutant at time point i.e. 70–80 h is partial and represents stationary phase of JP1.

Extraction of intracellular NADPH for HPLC

Bacterial cells grown to mid-log phase were suspended in a cell storage buffer (CSB; 50 mM Tris–HCl, 5 mM $MgCl_2$ and 1 mM phenylmethylsulfonylfluoride, pH 7.3), disrupted by sonication and subjected to centrifugation at 3000 × g to remove any intact cells. The cell-free extract (CFE) was then centrifuged for 3 h at 1 80 000 × g to obtain a soluble CFE fraction. Purity of the fraction was verified by monitoring G6PDH. For NADPH estimation, soluble CFE was diluted to 2 mg protein equivalent ml^{-1} in ddH_2O and then boiled for 2 min. Following removal of precipitate, the supernatant was injected in Agilent 1260 Infinity HPLC equipped with C_{18} reverse phase column (Agilent 5 HC-C18 (2) 250X4.6 mm) (Singh *et al*., 2008). HPLC protocol for separation and quantitation is described in Supporting Information Text S1.

Determination of intracellular concentration of acetyl-CoA

Acetyl-CoA extraction was conducted using the method described earlier with a few modifications. Cells (150 ml) grown in TSB broth until mid-log phase were harvested by centrifugation at 8000 × g for 10 min, resuspended in a mixture of 10 mM sodium phosphate (pH 7.5), 10 mM $MgCl_2$ and 1 mM EDTA were extracted with ice-cold perchloric acid (0.5 M $HClO_4$) for 40 min on ice with intermittent vortexing. The suspension was centrifuged for 5 min at 2800 × g and approximately 2 to 5 ml of supernatant was neutralized with saturated $KHCO_3$, concentrated by lyophilization to reduce the volume to 20% of the original (Lesley and Waldburger, 2003). HPLC protocol for separation and quantification is described in Supporting Information Text S1.

Assay of in vivo *role of chromomycin*

The subinhibitory concentration of chromomycin (Sigma) used for *in vivo* studies was 315 ng ml^{-1} for JP1. Determination of minimum inhibitory concentration (MIC) of chromomycin is presented in Supporting Information Text S1. Ascorbic acid was added at the final concentration of 200 μg ml^{-1}. Each of the two compounds was added to the culture at the start of the growth. At 40–46 h and 96–120 h, JP1 culture was withdrawn for plating, confocal microscopy and enzymatic assays.

Preparation of samples for RT-PCR for expression analysis of chromomycin biosynthesis genes

The protocol is as described previously (Kieser, 2000). Briefly, 10^8/ml of fresh spores were collected, pregerminated, and then inoculated in R2YE broth. Cultures were drawn at indicated time points (12 h, 17 h, 22 h, 27 h, 32 h, 38 h, 48 h, 60 h), were spun down and used for RNA extraction (RNA easy kit from Ambion) as described in Supporting Information Text S1.

Diamide and H_2O_2 sensitivity test

Equal number of spores (10^8/ml) of wild type was spread directly on surface of minimal agar medium containing glucose and that containing 1% of casamino acids. Different concentrations of each of diamide and H_2O_2 were placed in the wells created by cup borer. Zone of inhibition were examined after 36–48 h of incubation of plates at 30 °C.

Viability measurements

Cells were washed with 0.9% (w/v) NaCl and 20 μl of suspension was used for staining with LIVE/DEAD Bac-Light Bacterial Viability Kit (Molecular Probes) according to manufacturer instructions and observed under Leica TCSSP2-AOBS confocal laser-scanning microscope and LSM – 710 confocal microscope at wavelengths of 488 nm and 568 nm excitation and 530 nm (green) or 630 nm (red) emission (Manteca *et al*., 2005). Simultaneously, 0.1 ml of cultures was also plated on R2YE agar.

Acknowledgements

Divya Prajapati received financial support from ICMR, Govt. of India. Authors are thankful to DBT-MSUBILSPARE facility for Confocal microscopy. The authors declare no conflict of interest. The authors acknowledge Prof. Mervyn Bibb, John Innes Center, U.K., for suggestions during preparation of the manuscript. We also acknowledge the help of Dr. Maulik Thaker in the sequence analysis of chromomycin gene cluster.

References

Berg, J. M., Tymoczko, J. L., Stryer, L., Berg, J., Tymoczko, J., and Stryer, L. (2002) *Biochemistry: International Version (Hardcover)*. New York, NY: WH Freeman.

Berker, K. I., Güçlü, K., Demirata, B., and Apak, R. (2010) A novel antioxidant assay of ferric reducing capacity measurement using ferrozine as the colour forming complexation reagent. *Anal Methods* **2**: 1770–1778.

Borodina, I., Siebring, J., Zhang, J., Smith, C. P., van Keulen, G., Dijkhuizen, L., and Nielsen, J. (2008) Antibiotic overproduction in Streptomyces coelicolor A3 2 mediated by phosphofructokinase deletion. *J Biol Chem* **283**: 25186–25199.

Butler, M. J., Bruheim, P., Jovetic, S., Marinelli, F., Postma, P. W., and Bibb, M. J. (2002) Engineering of primary carbon metabolism for improved antibiotic production in *Streptomyces lividans*. *Appl Environ Microbiol* **68**: 4731–4739.

Chakraburtty, R., and Bibb, M. (1997) The ppGpp synthetase gene (relA) of Streptomyces coelicolor A3(2) plays a conditional role in antibiotic production and morphological differentiation. *J Bacteriol* **179**: 5854–5861.

Davies, J. (1990) What are antibiotics? Archaic functions for modern activities. *Mol Microbiol* **4**: 1227–1232.

Davies, J., Spiegelman, G. B., and Yim, G. (2006) The world of subinhibitory antibiotic concentrations. *Curr Opin Microbiol* **9**: 445–453.

Demain, A. L., and Fang, A. (2000) The natural functions of secondary metabolites. *Adv Biochem Eng Biotechnol* **69**: 1–39.

Fredriksson, A., and Nystrom, T. (2006) Conditional and replicative senescence in *Escherichia coli*. *Curr Opin Microbiol* **9**: 612–618.

Gomez-Escribano, J. P., Martin, J. F., Hesketh, A., Bibb, M. J., and Liras, P. (2008) *Streptomyces clavuligerus* relA-null mutants overproduce clavulanic acid and cephamycin C: negative regulation of secondary metabolism by (p)ppGpp. *Microbiology* **154**: 744–755.

Imlay, J. A. (2008) Cellular defenses against superoxide and hydrogen peroxide. *Annu Rev Biochem* **77**: 755–776.

Imlay, J. A. (2013) The molecular mechanisms and physiological consequences of oxidative stress: lessons from a model bacterium. *Nat Rev Microbiol* **11**: 443–454.

Jain, K. K. (2011) Neuroprotective agents. In *The Handbook of Neuroprotection*. Totowa, NJ: Humana Press, Springer, pp. 25–139.

Kalyanaraman, B., Darley-Usmar, V., Davies, K. J., Dennery, P. A., Forman, H. J., Grisham, M. B., *et al*. (2012) Measuring reactive oxygen and nitrogen species with fluorescent probes: challenges and limitations. *Free Radic Biol Med* **52**: 1–6.

Kamiyama, M. (1968) Mechanism of action of chromomycin A3. 3. On the binding of chromomycin A3 with DNA and physiochemical properties of the complex. *J Biochem* **63**: 566–572.

Kieser, T. (2000) *Practical Streptomyces Genetics*. Norwich, UK: John Innes Foundation.

Kraus, R. L., Pasieczny, R., Lariosa-Willingham, K., Turner, M. S., Jiang, A., and Trauger, J. W. (2005) Antioxidant properties of minocycline: neuroprotection in an oxidative stress assay and direct radical-scavenging activity. *J Neurochem* **94**: 819–827.

Leirós, M., Alonso, E., Sanchez, J. A., Rateb, M. E., Ebel, R., Houssen, W. E., *et al*. (2013) Mitigation of ROS insults by Streptomyces secondary metabolites in primary cortical neurons. *ACS Chem Nerosci* **5**: 71–80.

Lemire, J., Milandu, Y., Auger, C., Bignucolo, A., Appanna, V. P., and Appanna, V. D. (2010) Histidine is a source of the antioxidant, alpha-ketoglutarate, in *Pseudomonas fluorescens* challenged by oxidative stress. *FEMS Microbiol Lett* **309**: 170–177.

Lertvorachon, J., Kim, J. P., Soldatov, D. V., Boyd, J., Roman, G., Cho, S. J., *et al*. (2005) 1,12-Substituted tetracyclines as antioxidant agents. *Bioorg Med Chem* **13**: 4627–4637.

Lesley, J. A., and Waldburger, C. D. (2003) Repression of *Escherichia coli* PhoP-PhoQ signaling by acetate reveals a regulatory role for acetyl coenzyme a. *J Bacteriol* **185**: 2563–2570.

Lombo, F., Menendez, N., Salas, J. A., and Mendez, C. (2006) The aureolic acid family of antitumor compounds: structure, mode of action, biosynthesis, and novel derivatives. *Appl Microbiol Biotechnol* **73**: 1–14.

Mailloux, R. J., Lemire, J., and Appanna, V. D. (2011) Metabolic networks to combat oxidative stress in *Pseudomonas fluorescens*. *Antonie Van Leeuwenhoek* **99**: 433–442.

Manteca, A., Fernandez, M., and Sanchez, J. (2005) A death round affecting a young compartmentalized mycelium precedes aerial mycelium dismantling in confluent surface cultures of Streptomyces antibioticus. *Microbiology* **151**: 3689–3697.

Menendez, N., Nur-e-Alam, M., Brana, A. F., Rohr, J., Salas, J. A., and Mendez, C. (2004) Biosynthesis of the antitumor chromomycin A3 in *Streptomyces griseus*: analysis of the gene cluster and rational design of novel chromomycin analogs. *Chem Biol* **11**: 21–32.

Millan-Oropeza, A., Henry, C., Blein-Nicolas, M., Aubert-Frambourg, A., Moussa, F., Bleton, J., and Virolle, M. J. E. (2017) Quantitative proteomics analysis confirmed oxidative metabolism predominates in *Streptomyces coelicolor* versus glycolytic metabolism in *Streptomyces lividans*. *J Proteome Res* **16**: 2597–2613.

Nystrom, T. (1999) Starvation, cessation of growth and bacterial aging. *Curr Opin Microbiol* **2**: 214–219.

Nyström, T. (2004) Stationary-phase physiology. *Annu Rev Microbiol* **58**: 161–181.

Ochi, K. (2017) Insights into microbial cryptic gene activation and strain improvement: principle, application and technical aspects. *J Antibiot (Tokyo)* **70**: 25–40.

Price-Whelan, A., Dietrich, L. E., and Newman, D. K. (2006) Rethinking 'secondary' metabolism: physiological roles for phenazine antibiotics. *Nat Chem Biol* **2**: 71–78.

Price-Whelan, A., Dietrich, L. E., and Newman, D. K. (2007) Pyocyanin alters redox homeostasis and carbon flux through central metabolic pathways in *Pseudomonas aeruginosa* PA14. *J Bacteriol* **189**: 6372–6381.

Romano, A. H., and Nickerson, W. J. (1958) Utilization of amino acids as carbon sources by *Streptomyces fradiae*. *J Bacteriol* **75**: 161–166.

Rutledge, P. J., and Challis, G. L. (2015) Discovery of microbial natural products by activation of silent biosynthetic gene clusters. *Nat Rev Microbiol* **13**: 509–523.

Ryu, Y.-G., Butler, M. J., Chater, K. F., and Lee, K. J. (2006) Engineering of primary carbohydrate metabolism for increased production of actinorhodin in *Streptomyces coelicolor*. *Appl Environ Microbiol* **72**: 7132–7139.

Singh, R., Lemire, J., Mailloux, R. J., and Appanna, V. D. (2008) A novel strategy involved in [corrected] anti-oxidative defense: the conversion of NADH into NADPH by a metabolic network. *PLoS One* **3**: e2682.

Vining, L. C. (1990) Functions of secondary metabolites. *Annu Rev Microbiol* **44**: 395–427.

Xiao, Y., Wei, X., Ebright, R., and Wall, D. (2011) Antibiotic production by myxobacteria plays a role in predation. *J Bacteriol* **193**: 4626–4633.

Yim, G., Wang, H. H., and Davies, J. (2006) The truth about antibiotics. *Int J Med Microbiol* **296**: 163–170.

Supporting Information

Additional Supporting Information may be found in the online version of this article at the publisher's web-site:

Fig. S1. Restriction map and genetic organization of the partial biosynthetic gene cluster of Chromomycin. A. Restriction map of the cluster with respect to enzymes *BamH*I, *Bgl*II and *EcoR*I. B. The open reading frames and transcription directionality are represented as arrows, and their putative functions are described in Supporting Information Table S1C. The overlapping DNA present in different cosmid clones is indicated by a bold-line and the dotted lines indicate the tentative limits of insert DNA in each clone. The boxed portion in the cosmid #2.19 corresponds to the DNA deleted from the genome of the mutant JP1.

Fig. S2. Genetic evidence for accuracy of the deletion of PKS DNA in the JP1. (I) Restriction enzyme sites for *BamHI* are shown encasing the deletion joint point marked by the unique *BglII* site with the plasmid pGMΔ*Pst* present at that site in the chromosome of JP1; (II) Predicted structure of the plasmid retrieved from the chromosome of JP1 following *Bgl*II (A) and *BamH*I (B) digestion of genomic DNA of JPI. (III) RE analysis of the retrieved plasmid: Lane 1- *Bgl*II digestion of plasmid (retrieved from JP1 mutant following *BamH*I digestion and religation) releases 2.284 Kb DNA encompassing deletion joint point.; Lane 2- The *BamH*I fragment including the deletion joint point is cloned in pBluescript KS vector from #2.19Δ*Bgl* and released with *BamH*I restriction digestion; Lane 3- Lambda *Hind*III marker; Lane 4- *EcoR*I + *Pst*I digestion of pGMΔ*Pst* plasmid recovered from JP1 (following *Bgl*II digestion and intramolecular religation) and Lane 5 – The *EcoR*I + *Pst*I digestion original pGMΔ*Pst* vector DNA (IV) Southern hybridization of JP1 chromosomal DNA using pGMΔ*Pst* as a probe. Left: agarose gel of the *BamH*I and *Bgl*II digestion of JP1 genomic DNA; Right: Southern hybridization of the aforementioned blot.

Fig. S3. HPLC analysis of extracts for chromomycin production. HPLC analysis of extract of wild type (I); JP1 (II) and integrant (JP1+ #2.19) (III). The retention times are indicated for chromomycin A1 (22 min.), A2 (25 min.) and A3 (28 min.).

Fig. S4. NADPH estimation by HPLC. Intracellular levels of NADPH in WT and JP1 as measured by HPLC.

Fig. S5. Acetyl Co-A estimation by HPLC. Intracellular levels of Acetyl Co-A in WT and JP1 as measured by HPLC.

Table S1. List of genes of chromomycin biosynthetic cluster from gene bank accession number KC249518.1*

Table S2. List of strains and plasmids used

Table S3. List of primer pairs used for RT-PCR analysis